

# Quantitative Susceptibility Mapping of Hemorrhages in TBI Using the 3D multi-echo Gradient Echo MRI at 3T

Haiying Tang<sup>1</sup>, Tian Liu<sup>2</sup>, Wei Liu<sup>3</sup>, Hai Pan<sup>3</sup>, Reed Selwyn<sup>1</sup>, Terry Oakes<sup>4</sup>, Yi Wang<sup>2</sup>, and Gerard Riedy<sup>4</sup>

<sup>1</sup>Radiology, Uniformed Services University of the Health Sciences, Bethesda, MD, United States, <sup>2</sup>Biomedical Engineering, Cornell University, New York, NY, United States, <sup>3</sup>Center for Neuroscience and Regenerative Medicine, Henry M Jackson Foundation, Bethesda, MD, United States, <sup>4</sup>National Intrepid Center of Excellence, Walter Reed National Military Medical Center, Bethesda, MD, United States

**Introduction** In the military, the Iraq and Afghanistan wars have potentially exposed more than 300,000 soldiers to mild traumatic brain injury (TBI), with more than 45,000 soldiers diagnosed with TBIs. The true incidence of TBI in the military is unknown since many cases, especially mild TBI, will have negative findings using typical clinical imaging protocols. Diagnosis of TBI with high sensitivity and specificity is a top priority for military medicine. Diffuse axonal injury (DAI), marked by petechial hemorrhage, is a trademark brain injury following blast-induced and acceleration brain movements and is not observable using conventional MRI or CT. Yet, susceptibility weighted imaging (SWI) [1-2] and quantitative susceptibility mapping (QSM) [3-4] can detect and quantify petechial hemorrhages, micro-bleeds, iron deposition, and calcifications that may predict DAI. We hypothesize that QSM will provide new information that is not obtained using other quantitative imaging, such as diffusion tensor imaging (DTI), which is quickly becoming the de facto standard for TBI imaging.

**Methods** Healthy volunteers (n=6) and TBI patients (n=100) were examined under an Institutional Review Board approved protocol. 16 patients with micro-bleeds seen from SWI were analyzed in the study. The MR measurements including volumetric T<sub>1</sub>, T<sub>2</sub>, SWI, DTI, and FLAIR (before and after Gd-DPTA injection) imaging were performed at Walter Reed Army Medical Center (WRAMC) and National Intrepid Center of Excellence (NICoE), using the GE 3T whole body MR scanner (GE750 Systems, GE Healthcare, Milwaukee, WI) equipped with the 32-channel phased array head coil.

SWI was implemented using a 3D flow-compensated multi-echo gradient-echo sequence, with TR=45ms, 5 echoes, TE0=13ms, echo-spacing 6ms, flip-angle=20°, BW=62.5 kHz, and asset-factor=2. Images were acquired with a 512×256 matrix, 24×24 cm<sup>2</sup> FOV, and 90 slices at 1.5mm thickness. This yielded entire brain coverage within a clinically acceptable scan time (5'30"). DTI is acquired with 2mm<sup>3</sup> isotropic resolution and 48 diffusion directions. SWI images were processed based on the magnitude and phase information [1] obtained at each individual echo time, using the SPIN software (HUH-MR Research Radiology, Wayne State Univ., Detroit, MI). SWI at TE=25ms were selected for radiologist review. R<sub>2</sub>\* (relaxation rates) were calculated by exponential fitting to the 5-echo images.

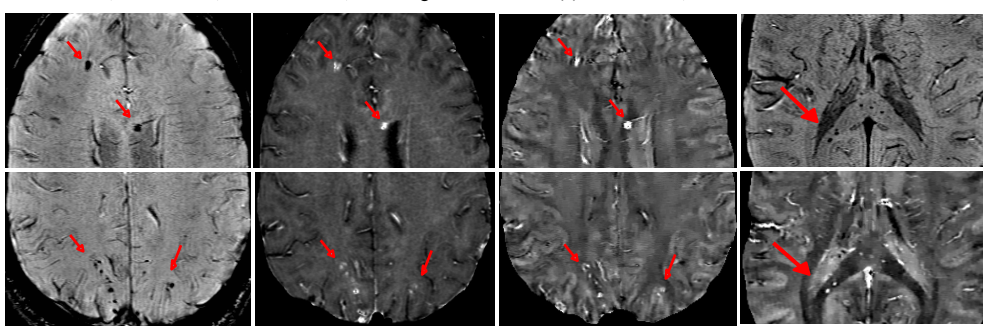
QSM images were processed based on the multi-echo complex imaging data, using the morphology-enabled dipole inversion approach [3-4], which is implemented in the MEDI software (Dept. of Biomedical Engineering, Cornell University, NY). The reconstruction of QSM images from the measured complex phase data is an ill-posed inverse problem. MEDI formulates the inverse problem as a weighted L1 minimization problem. Among all the candidate solutions, the estimated susceptibility distribution x\* is the one with the sparsest difference between its edges and those from the anatomic image. This spatial prior helps to eliminate solutions with spurious edges resulting from the streaking artifacts often seen in QSM [5] and determines a solution that is physically meaningful.

Comparisons were made between SWI and T<sub>1</sub>W/T<sub>2</sub>W/FLAIR images, and QSM and R<sub>2</sub>\*/ADC/ FA measurements in sampled brain regions (white matter, splenium corpus callosum, caudate, globus pallidus, putamen, thalamus, red nucleus, and choroid plexus, etc.), hemorrhages, and micro-bleeds in TBI patients.

**Results** Figure 1a-c show scattered hemorrhages (indicated by red arrows) in the white matter in 2 SWI (negative contrast) and QSM (positive contrast) images in a patient with moderate TBI (4 weeks post injury). A deep white matter micro-bleed is noted in the left body of corpus callosum (Fig. 1c). Micro-bleeds are also clearly detectable in the splenium corpus callosum in another patient with mild TBI (Fig. 1d, 4 month post injury). The heterogeneity of the QSM in different brain regions and in different hemorrhage sites demonstrate the complexity of iron deposition in these areas. White matter is diamagnetic, thus has negative QSM values. The splenium corpus callosum contains high density of axons, and its mean QSM is around -30 to -40 ppb which is lower than the average of the white matter (-10 to -20 ppb). Because of this, good contrast is shown when there are micro-bleeds in the splenium corpus callosum. The size of the hemorrhages and the intensity of QSM in these hemorrhagic regions were calculated using the histogram of QSM. The total QSM of the hemorrhages can be the sum of the positive QSM in the area. Patient 1 has a broader spread area of DAI (144.3ppm, with a total volume of 65mm<sup>3</sup>, Fig. 1c) than that of the Patient 2 (14.5ppm, with a total volume of 6.5mm<sup>3</sup>, Fig. 1f). With co-registration of QSM and FA/ADC (calculated from DTI) maps, QSM were compared with FA and R<sub>2</sub>\* in white matter, corpus callosum, hemorrhages, and other brain regions (Fig. 2a). White matter (gray dots) has a broader range of FA (0.4~0.9). The FA of the white matter hemorrhages in patient 1 (orange dots, n=20, mean FA 0.4) are smaller compared to that of the contralateral white matter samples (green triangle, n=20, mean FA 0.51), confirmed an axonal injury in the area. The FA in the micro-bleeds in splenium corpus callosum in patient 2 (brown square) didn't change compared to the FA in the splenium corpus callosum (green diamond). There are no changes of ADC in hemorrhages. QSM and R<sub>2</sub>\* sampled in various brain regions and hemorrhages are well correlated (Fig. 2b), and QSM can better differentiate calcified areas compared to R<sub>2</sub>\*. The tissue classification using the QSM and DTI measurements, and the correlation between the neuropsychological data and the scoring scheme based on the QSM and location of injury for all patients (n=16) are under investigation.

**Conclusions and discussions** SWI is sensitive in detection of micro-bleeds and in diagnosis of DAI. SWI images generated at different echo times can be used to characterize venous structures and traumatic lesions. Smaller venous structures and micro-bleeds are clearly visible at longer echo time. SWI derived from shorter echoes provides reasonable lesion contrast with less off-resonance artifact and signal drop out. R<sub>2</sub>\* can be limited by signal drop out. The local susceptibility measurement by using QSM is independent of echo times [4]. QSM removes blooming artifacts in T<sub>2</sub>\* hypointensity, and offers more accurate detections and measures of blood products, hemorrhages, micro-bleeds, venous deoxyhemoglobin, and calcifications compared to the R<sub>2</sub>\*. QSM provides a localized axonal injury assessment combining DTI measurement. **QSM analysis is not limited to white matters.** More TBI patients (from mild to moderate) will be included in the QSM analysis, and the relationship between QSM imaging markers and clinical outcomes will be investigated, to evaluate the potentiality of SWI/QSM in characterization of TBI and DAI.

**Reference** 1. Haacke EM, Mittal S, Wu Z, et al. AJNR Am J Neuroradiol 30: 19-30, 2009. 2. Haacke EM, Xu Y, Cheng YN, et al. Magn. Reso. Med. 52:612-618, 2004. 3. de Rochefort L, Liu T, Kressler B, et al. Magn. Reso. Med. 63: 194-206, 2010. 4. Liu T, Surapaneni K, Lou M, et al. Radiology, Number? , 2011. 5. Shmueli K , de Zwart JA , van Gelderen P , et al. Magn. Reso. Med. 62(6): 1510 – 1522, 2009.



(a) SWI (no mIP), Patient 1 (b) R<sub>2</sub>\* map, Patient 1 (c) QSM, Patient 1 (d) SWI(up)/QSM, Patient 2

Figure 1. SWI and QSM are more sensitive to detect hemorrhages and micro-bleeds

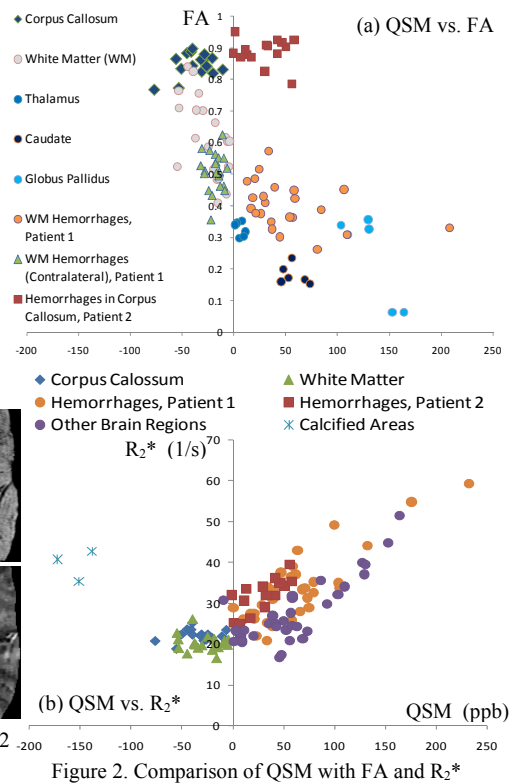


Figure 2. Comparison of QSM with FA and R<sub>2</sub>\*